

1 **Hierarchical S-doped Porous Carbon Derived from By-products**

2 **Lignin for High-Performance Supercapacitors**

3 Jingyang Tian, Zhangming Liu, Zhenghui Li, Wenguang Wang, Haiyang Zhang*

4 College of Materials and Energy, Guangdong University of Technology, Guangzhou

5 51006, China

6

7

8

9

10

11

12

13

14

15

16

17

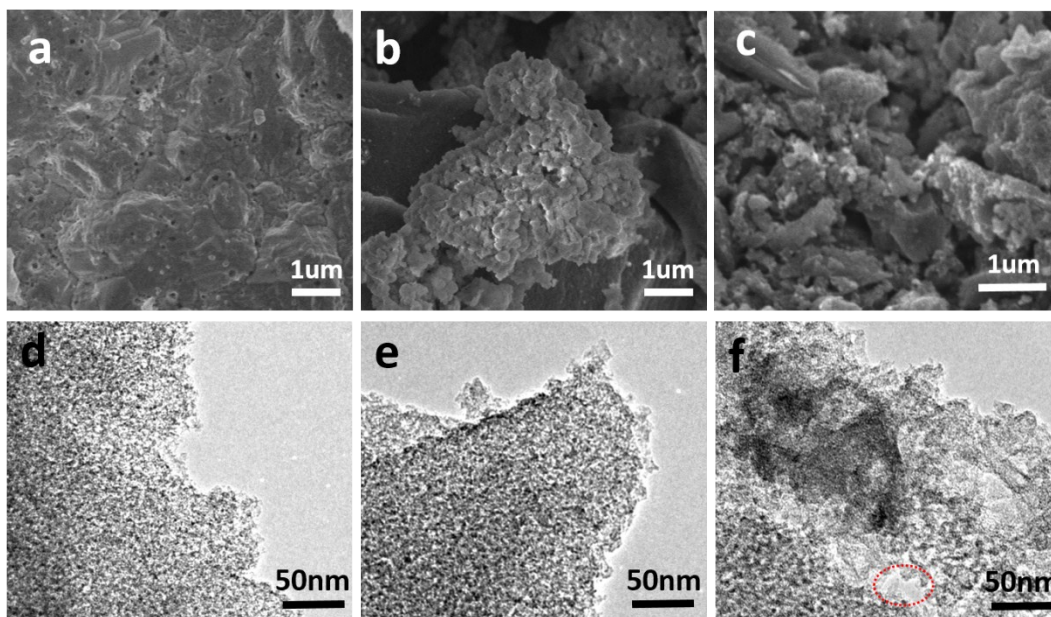
18

19

20

21

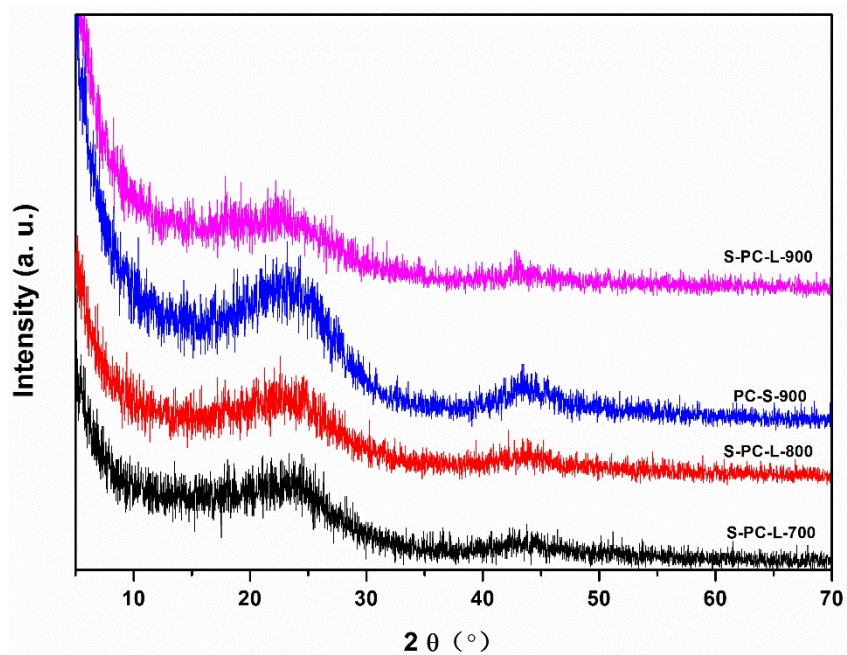
22



23

24 Figure S1. (a) FE-SEM image of PC-S-900. (b) FE-SEM image of S-PC-L-700. (c) FE-SEM image of S-PC-L-800

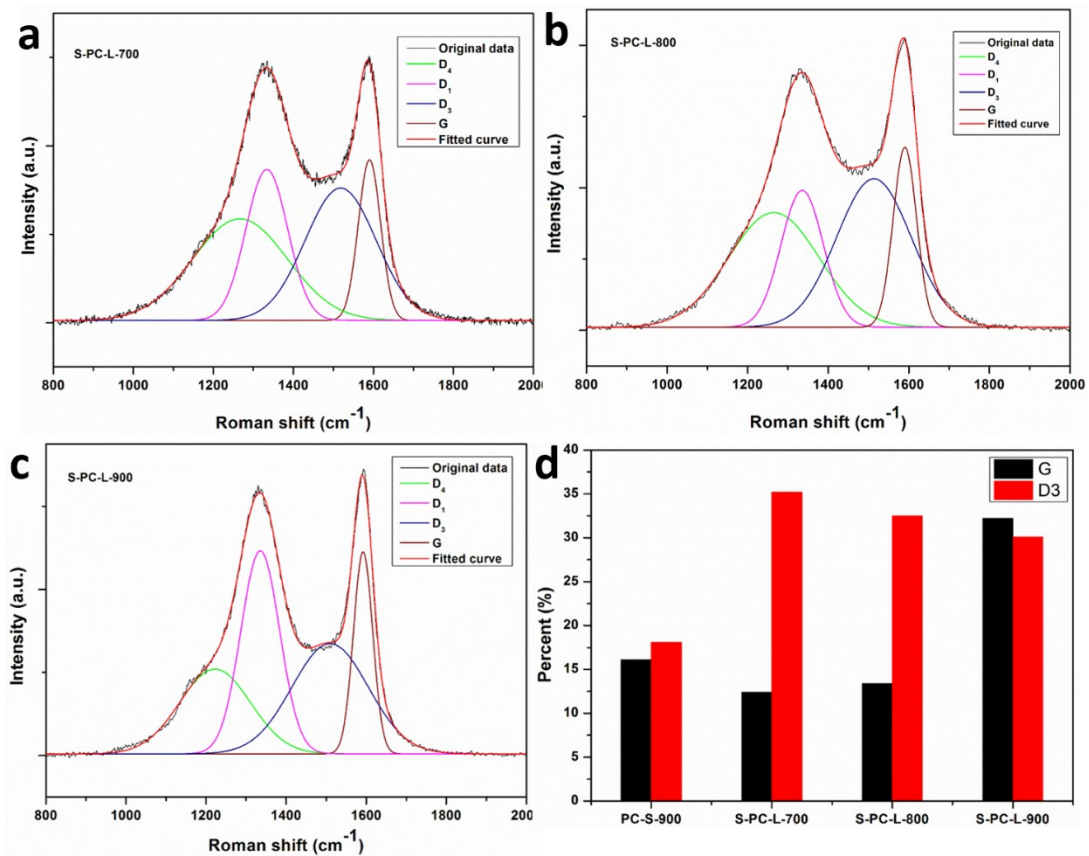
25 (d) FE-TEM image of PC-S-900. (e) FE-TEM image of S-PC-L-700. (f) FE-TEM image of S-PC-L-800.



26

27

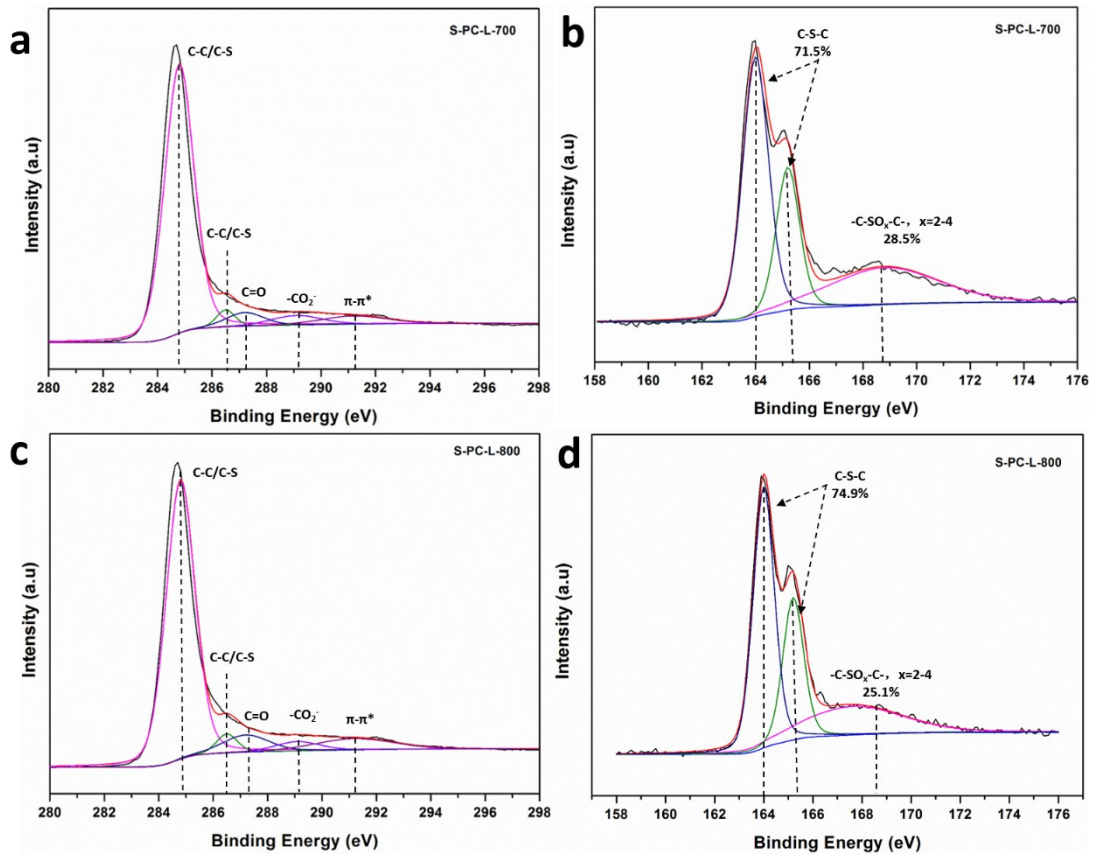
Figure S2. XRD patterns of samples.



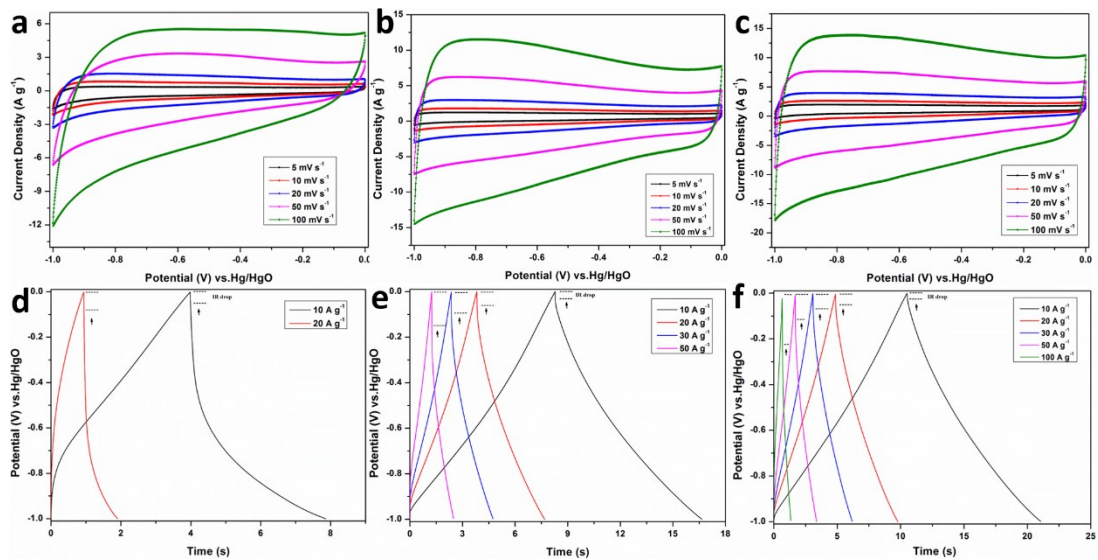
28

29 Figure S3. (a) Raman spectra of (a) S-PC-L-700, (b) S-PC-L-800, (c) S-PC-L-900, and (d) percent of amorphous
 30 and ideal graphitic carbon.

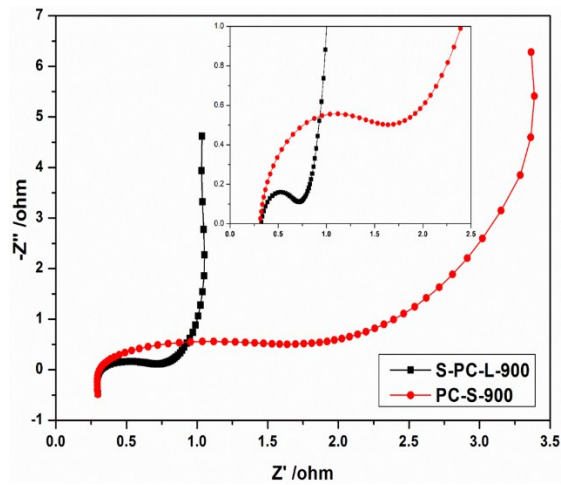
31



32
 33 Figure S4. (a) High resolution XPS spectra of C 1s (a) and S 2p (b) of S-PC-L-700, C 1s (c) and S 2p (d) of S-PC-
 34 L-800.



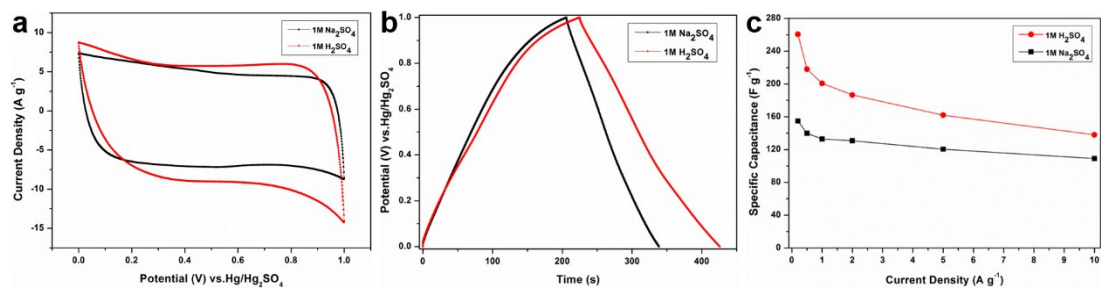
35
 36 Figure S5. The CV curves of the (a) S-PC-L-700, (b) S-PC-L-800 and (c) PC-S-900 at various scan rates. The
 37 galvanostatic charge-discharge curves of (d) S-PC-L-700, (e) S-PC-L-800 and (f) PC-S-900 at various current
 38 densities.



39

40

Figure S6. Nyquist plots of PC-S-900 and S-PC-L-900.



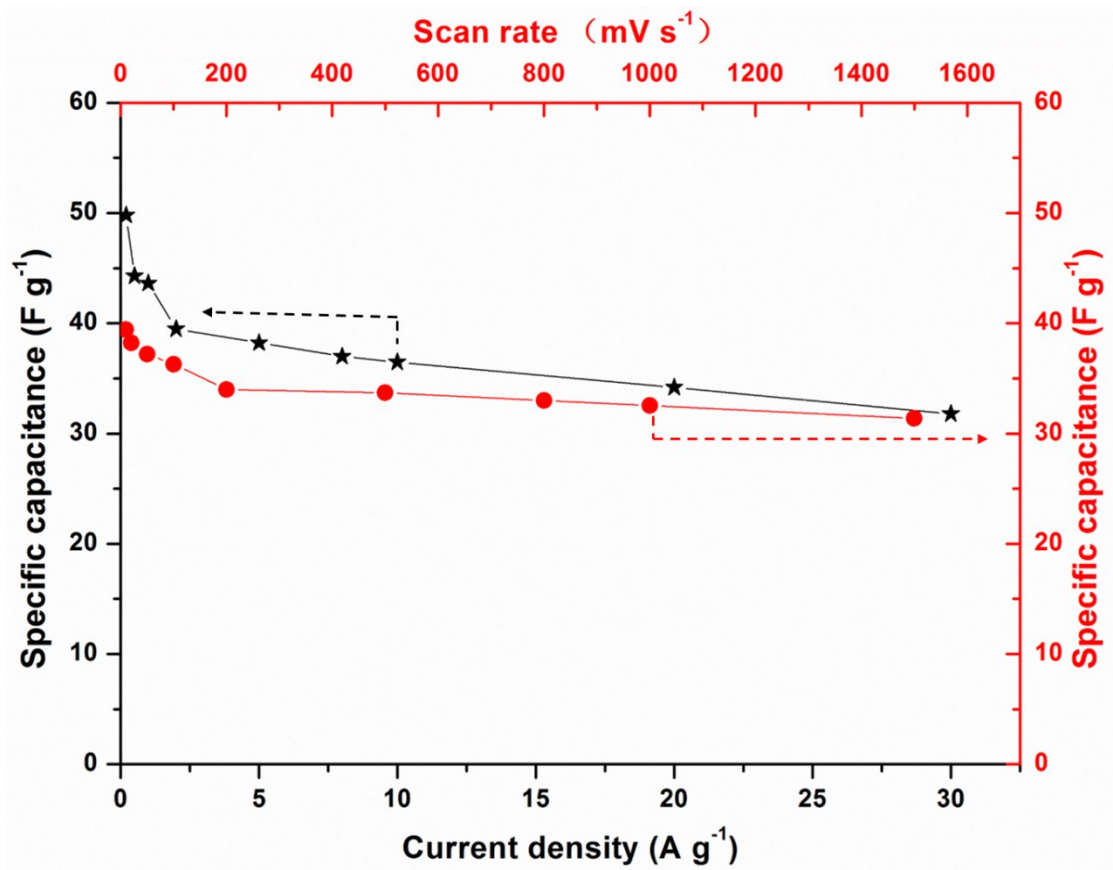
41

42 Figure S7. Electrochemical performance of the S-PC-L-900 in 1 M H₂SO₄ and Na₂SO₄ aqueous electrolyte in a

43 three-electrode system. (a) CV curves at 50 mV s⁻¹, (b) galvanostatic charge-discharge curves at 1 A g⁻¹, (c)

44 specific capacitance at various current densities.

45



46

47

Figure S8. Specific capacitance of S-PC-L-900 symmetric supercapacitor calculated from cyclic voltammetry

48

curves and GCD curves.